Independent Amplitude and Phase Control of Two Orthogonal Linearly Polarised Light and Its Applications

Hao Chen, *Member, IEEE*, and Erwin H. W. Chan, *Senior Member, IEEE*

***Abstract*—A technique to provide independent control on the amplitude and phase of two orthogonal linearly polarised light is presented. It is based on operating a commercial dual-polarisation dual-drive Mach Zehnder modulator (DPol-DDMZM) in reverse direction that routes the input light in slow and fast axis into two different DDMZMs. The technique has the advantage of controlling the phase of the slow-axis light and the amplitude of the fast-axis light has no effect on the light travelling in the orthogonal polarisation state. It has applications in linearised microwave photonic links, frequency multipliers and microwave phase shifters. A new microwave photonic Hilbert transformer based on using the reverse operating DPol-DDMZM to alter the phase of an RF modulation sideband without affecting the orthogonally polarised optical carrier is developed. Experimental results demonstrate 24.3 dB attenuation in the fast-axis light with no change in the slow-axis light, and 0°–360° RF phase shift for only 3.3 V change in DC voltage. The new Hilbert transformer with less than 2.5° phase imbalance and 0.4 dB amplitude ripples over 4–18 GHz frequency range is also demonstrated.**

***Index Terms*—Optical modulators, microwave photonics, phase shifter, Hilbert transformer, orthogonal polarisation state.**

I. Introduction

PHOTONIC techniques for processing and measuring microwave signals are attractive as they have the potential for wideband operation, immunity to electromagnetic interference, wide tunability and high reconfigurability [1], [2]. An electro-optic modulator is a curial component in many microwave photonic devices. It is not only used to convert a microwave signal into an optical domain for signal transmission but to generate optical frequency components with desired amplitudes, frequencies and phases for microwave signal processing and measurement. Launching a light with a 45° angle to the slow axis into a polarisation modulator or a phase modulator can produce optical frequency components in two orthogonal polarisation states. Two orthogonal linearly polarised optical signals can also be generated by a dual-polarisation dual-drive Mach Zehnder modulator (DPol-DDMZM) or a dual-polarisation dual-parallel Mach Zehnder modulator (DPol-DPMZM).

Manuscript received August 25, 2021; revised October 13, 2021; accepted October 18, 2021. Date of publication October 20, 2021; date of current version November 3, 2021. *(Corresponding author: Erwin Chan.)*

The authors are with the College of Engineering IT and Environment, Charles Darwin University, Darwin, NT 0909, Australia (e-mail: simonchenhao@hotmail.com; erwin.chan@cdu.edu.au).

Digital Object Identifier 10.1109/JPHOT.2021.3121655

A number of microwave photonic devices have been developed based on controlling the amplitude and phase of two orthogonal linearly polarised optical signals. For example, by designing the amplitude of two orthogonal polarisation signals, the third order intermodulation distortion in a microwave photonic link can be suppressed [3], [4] and a frequency multiplier can be realised [5]. Microwave photonic phase shifters can also be implemented by controlling the phase of two orthogonal linearly polarised optical signals [6], [7]. There are several techniques to control the amplitude and phase of two orthogonal polarisation signals. These include using an adjustable linear polariser [3], [4], adjusting the light polarisation state via a polarisation controller (PC) in front of a polariser [4], [6], and applying a DC voltage to a phase modulator that supports phase modulation in both the transverse magnetic (TM) mode and the transverse electric (TE) mode with different phase modulation indices [7]. These techniques have the problem of changing the characteristic of the light in one polarisation state also affects the light travelling in the orthogonal polarisation state. This can be seen in [7] where a Z-cut $LiNbO_3$ phase modulator, which has a polarisation dependent switching voltage, is used to alter the phase difference of two orthogonal polarisation signals. Applying a DC voltage to this phase modulator not only changes the phase of the light in slow axis but also changes the phase of the light in fast axis by a different amount. Hence a large DC voltage change is needed to obtain a full 0°–360° RF phase shift range. It is desirable to have a device that provides independent amplitude and phase control on two orthogonal linearly polarised optical signals from the same or different optical sources. However, to our knowledge, such device has not been reported.

The purpose of this paper is to present a new technique to independently control the amplitude and phase of two orthogonal linearly polarised optical signals. It is based on operating a DPol-DDMZM in reverse direction. Applying a DC voltage to a DDMZM inside the DPol-DDMZM can alter the phase of the input light in slow axis without affecting the input light in fast axis. Similarly applying a DC voltage to the other DDMZM can alter the amplitude of the input light in fast axis with no change in the input slow-axis light. In addition to provide independent amplitude and phase control, the reverse operating DPol-DDMZM converts two orthogonal polarisation signals to have the same polarisation state. A new microwave photonic Hilbert transformer is developed using the proposed amplitude and phase controller (APC). It does not require high-frequency electrical components

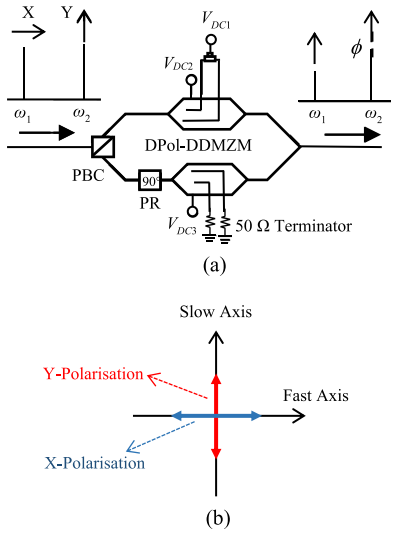

Fig. 1. (a) New microwave photonic based amplitude and phase controller (APC). → and ↑ represent the X and Y polarisation state respectively. ϕ represents the phase change. (b) X-polarisation light wave aligned to the fast axis and Y-polarisation light wave aligned to the slow axis. PR: polarisation rotator; PBC: polarisation beam combiner.

and hence it has very little amplitude and phase imbalance over a wide operating frequency range. Experimental results are presented that demonstrate independent amplitude and phase controls of two orthogonal linearly polarised optical signals using the APC. Broadband quadrature-phase outputs in the new microwave photonic Hilbert transformer is also demonstrated.

II. Operation Principle and Simulation Results

A new microwave photonic structure, which provides independent control on the amplitude and phase of two orthogonal linearly polarised light, is shown in Fig. 1. It is based on a commercial DPol-DDMZM (Fujitsu FTM7980) operating in reverse direction. The input of the reverse operating DPol-DDMZM is two orthogonal linearly polarised light with angular frequencies ω_1 and ω_2. The two X and Y polarisation light waves are travelled in the fast and slow axis respectively as shown in Fig. 1(b). The polarisation beam combiner (PBC) inside the DPol-DDMZM acts as a polarisation beam splitter (PBS). The Y-polarisation light in the slow axis is routed to the top DDMZM, which has two RF ports and a DC port. A DC voltage V_{DC1} is equally split into two via a tee connector before injecting into the two DDMZM RF ports. Another DC voltage V_{DC2} is applied to the DDMZM DC port to bias the modulator at the peak point. Note that a DDMZM behaves as a phase modulator when it is biased at the peak point and is driven by two identical signals [8], [9]. Here an optical phase shifting operation is obtained as two identical DC voltages into the two modulator RF ports. There is no velocity mismatch problem [10] since only DC voltages are applied to the RF ports of a reverse operating DDMZM. Therefore the phase of the Y-polarisation light can be controlled by the DC voltage V_{DC1}. The X-polarisation light in the fast axis at the APC input is routed to the bottom path of the DPol-DDMZM. The 90° polarisation rotator in the bottom path rotates the light polarisation state by 90° so that it travels in the slow axis before entering the bottom DDMZM. The RF ports of this DDMZM are terminated by 50 Ω terminators. The amplitude of the light passing through the bottom DDMZM can be controlled by the DC voltage V_{DC3} into the modulator DC port. The light travelled in the top and bottom paths of the DPol-DDMZM are combined by a 3-dB coupler. The output of the structure shown in Fig. 1 is two light waves travelling in the slow axis where their phase and amplitude can be independently controlled by V_{DC1} and V_{DC3} respectively.

Let's consider the case where the input of the APC consists of two different-wavelength light waves with orthogonal polarisation states from two optical sources, the APC input electric field is given by

$$E_{in}(t) = E_1 e^{j\omega_1 t}\hat{x} + E_2 e^{j\omega_2 t}\hat{y} \tag{1}$$

where E_1 and E_2 are the electric field amplitude of the two light waves into the APC, $\omega_1 = 2\pi f_1$ and $\omega_2 = 2\pi f_2$ are the angular frequency of the two light waves, and $\hat{x}$ and $\hat{y}$ represent the two orthogonal linearly polarisation states. The electric field at the output of the APC can be expressed as

$$E_{out}(t) = E_1 e^{j\omega_1 t}\frac{1}{2\sqrt{2}}\sqrt{t_{ff2}}\left(1+e^{j\beta_3}\right) + E_2 e^{j\omega_2 t}\frac{1}{\sqrt{2}}\sqrt{t_{ff1}}e^{j\beta_1} \tag{2}$$

where $t_{ff1(2)}$ is the insertion loss in the top (bottom) path of the reverse operating DPol-DDMZM, $\beta_1 = \pi V_{DC1}/V_{\pi,RF}$, $V_{\pi,RF}$ is the DDMZM RF port switching voltage, $\beta_3 = \pi V_{DC3}/V_{\pi,DC}$ and $V_{\pi,DC}$ is the DDMZM DC port switching voltage. (2) shows changing V_{DC1} alters the phase of the Y-polarisation light without affecting the X-polarisation light, and changing V_{DC3} alters the amplitude of the X-polarisation light. Since the two light waves are from two different optical sources, they are incoherent. At the output of the APC, the optical power of the light with angular frequency of ω_1 and ω_2 are $0.25{E_1}^2 t_{ff2}(1+\cos\beta_3)$ and $0.5{E_2}^2 t_{ff1}$ respectively. This shows the power of the X-polarisation light travelling in the fast axis into the APC can be controlled by the bottom DDMZM bias angle β_3 while the power of the Y-polarisation light remains unchanged. Note that although using a reverse operating DPol-DDMZM to control the light amplitude has been proposed, there is no theoretical analysis to support to the experimental observation [11].

In the case where the input of the APC consists of a X-polarisation optical carrier and a Y-polarisation RF modulation sideband generated by a DPol-DDMZM or a DPol-DPMZM followed by an optical filter [7], [12]. The electric field at the input and output of the APC are given by

$$E_{in}(t) = E_c e^{j\omega_c t}\hat{x} + E_s e^{j(\omega_c+\omega_{RF})t}\hat{y} \tag{3}$$

and

$$E_{out}(t) = E_c e^{j\omega_c t}\frac{1}{2\sqrt{2}}\sqrt{t_{ff2}}\left(1+e^{j\beta_3}\right) + E_s e^{j(\omega_c+\omega_{RF})t} \times \frac{1}{\sqrt{2}}\sqrt{t_{ff1}}e^{j\beta_1} \tag{4}$$

where E_s and E_c are the electric field amplitude of the RF modulation sideband and the optical carrier at the APC input respectively, and $\omega_c = 2\pi f_c$ and $\omega_{RF} = 2\pi f_{RF}$ are the angular frequency of the optical carrier and the input RF signal respectively. (4) shows the phase of the RF modulation sideband can be controlled by β_1. The output of the APC is detected by a photodetector. A photocurrent at the RF signal frequency is generated at the photodetector output. It can be obtained from the product of the photodetector responsivity $\Re$ and the absolute square of the APC output electric field given in (4), which can be written as

$$I_{RF}(t) = \Re E_s E_c \sqrt{t_{ff1}}\sqrt{t_{ff2}} \cos\left(\frac{\beta_3}{2}\right) \times \cos\left(\omega_{RF} t + \beta_1 - \frac{\beta_3}{2}\right) \quad (5)$$

It can be seen from (5) that a continuous 0° to 360° RF signal phase shift can be obtained by a total of $2V_{\pi,RF}$ changes in the DC voltage V_{DC1}. Note that the output RF signal amplitude can be controlled by the bottom DDMZM bias angle β_3. Changing the bottom DDMZM bias angle β_3 also changes the output RF signal phase but the change can be compensated by adjusting V_{DC1}. These RF signal amplitude and phase control functions are useful in phased array antenna systems [13]. Since the DDMZM RF ports have a wide bandwidth, fast beam steering can be realised by sweeping the DC voltage V_{DC1} into the DDMZM RF ports to alter the RF signal phase. As in all electro-optic intensity modulators, the proposed APC based on two DDMZMs connected in parallel has the bias drift problem [14]. Drift in the modulator operating point alters the amount of attenuation and phase shift introduced by the APC on the two orthogonal linearly polarised optical signals. Commercial modulator bias controllers can be incorporated into the APC to obtain a long-term stable performance.

Fig. 2(a) shows the output RF signal power attenuation versus the bottom DDMZM bias angle β_3. The corresponding change in the output RF signal phase is also shown in the figure. The figure shows, as the bias angle increases, the attenuation increases, and the output RF signal phase is changed from 0° to -90° when changing the bias angle from 0° to 180°. Fig. 2(b) shows the DC voltage V_{DC1} into the RF port of the top DDMZM required to obtain different RF signal phase shifts for a DDMZM RF port switching voltage of 1.7 V. This shows a full 360° phase shift can be obtained by having a total of 3.4 V change in V_{DC1} for different amounts of RF signal attenuation.

The proposed APC has a number of applications. It can be used to replace the adjustable linear polariser in [4] to suppress the third order intermodulation distortion in a microwave photonic link. It can be used to replace the PC and the linear polariser in [6], or the phase modulator that supports phase modulation in both TM and TE modes in [7] to realise microwave phase shifting operation. Additionally, the reverse operating DPol-DDMZM based APC can be used to implement a microwave photonic Hilbert transformer as shown in Fig. 3. A Hilbert transformer is a device that takes an RF signal and generates two equal-amplitude

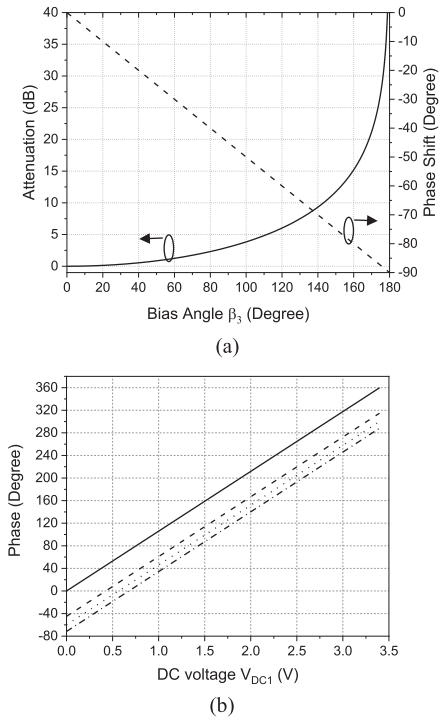

Fig. 2. (a) Output RF signal attenuation (solid line) as a function of the bias angle β_3 for $\beta_1 = 0$, and the corresponding output RF signal phase shift (dashed line). (b) Output RF signal phase shift versus the DC voltage V_{DC1} into the DDMZM RF port for $V_{\pi,RF}$= 1.7 V when the bias angle β_3 is set to obtain 0 dB (solid), 3 dB (dashed), 6 dB (dotted) and 10 dB (dashed-dotted) output RF signal attenuation.

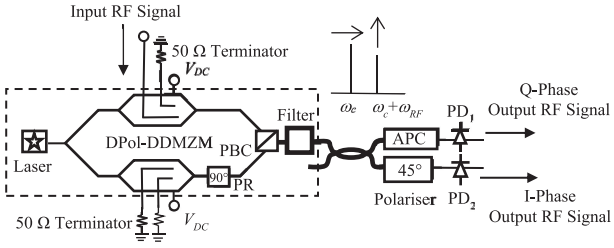

Fig. 3. New all-optical Hilbert transformer based on the proposed amplitude and phase controller. The bold lines represent polarisation maintaining components. PR: polarisation rotator; PBC: polarisation beam combiner.

quadrature-phase RF signals [1]. It is widely used in communication and electronic warfare systems. A microwave photonic Hilbert transformer can be implemented using a delay line technique [15]. However, it has a complex structure as it requires several optical sources with specific powers and wavelengths, and a dispersive fibre. Furthermore, the delay line based Hilbert transformer involves high-frequency electrical components and its performance degrades at frequencies above 20 GHz. A Hilbert transformer implemented using a Fourier-domain optical processor (FD-OP) is free of electrical components and has small amplitude and phase imbalance [16]. However, a FD-OP is bulky and costly.

The components in the dashed box in Fig. 3 are a laser source, a DPol-DDMZM and an optical filter. The input RF signal is

applied to an RF port of a null-biased DDMZM. The other DDMZM with 50 Ω terminators in the RF ports is biased at the peak point. The optical filter at the DPol-DDMZM output filters out the lower RF modulation sideband. Hence the structure inside the dashed box in Fig. 3 produces an optical carrier and an upper RF modulation sideband in orthogonal polarisation states. An optical coupler splits the optical signals into two where one passes through the APC and the other passes through a polariser with a 45° angle to the slow axis before detecting by photodetectors (PD_1 and PD_2). Note that the optical filter and the optical coupler need to be polarisation maintaining to ensure the carrier and sideband are travelled in the fast and slow axis respectively, before entering the APC and the 45° linear polariser. By setting the DC voltages into the APC so that $\beta_1 = \pi/2$ and $\beta_3 = 0$, PD_1 output RF photocurrent can be expressed as

$$I_{PD1,RF}(t) = \Re E_s E_c \sqrt{t_{ff1}} \sqrt{t_{ff2}} (1-\alpha) \cos\left(\omega_{RF} t + \frac{\pi}{2}\right) \quad (6)$$

where α is the optical coupler coupling ratio. PD_2 output RF photocurrent can be written as

$$I_{PD2,RF}(t) = 2\Re E_s E_c \alpha \cos(\omega_{RF} t) \quad (7)$$

This (6) and (7) show the two output RF signals have a 90° phase difference and their amplitude can be the same by designing the optical coupler coupling ratio. Note that the PBC in the APC acts as a PBS to split two orthogonal linearly polarised optical signals and a practical PBC/PBS has a finite polarisation extinction ratio. The Hilbert transformer shown in Fig. 3 was set up in a photonic simulation software to examine the effect of the PBC polarisation extinction ratio on the Hilbert transformer performance. Simulation results show the Hilbert transformer has 0.8° phase imbalance and less than 0.1 dB amplitude imbalance when the PBC in the APC has 25 dB polarisation extinction ratio. The phase and amplitude imbalance increase to 7.3° and 0.5 dB respectively, for a 15 dB polarisation extinction ratio PBC.

The new Hilbert transformer does not require high-frequency electrical components. It has a wide bandwidth as its upper and lower operating frequencies are only limited by the modulator bandwidth and the steepness of the amplitude response edges of the optical filter used to remove the lower sideband. Using a high edge roll-off optical filter enables the Hilbert transformer to be operated from few GHz to tens of GHz. Since the 90° phase difference between the two outputs is introduced by the DC voltage V_{DC1} into the APC, it is independent to the RF signal frequency. V_{DC1} can also be accurately adjusted to minimise the phase imbalance in the two quadrature-phase outputs. The components used to implement the Hilbert transformer including the DPol-DDMZM, the optical filter which can be implemented using a fibre Bragg grating [17], the optical coupler, the APC and the polariser can be integrated and packaged into a compact device. The new all-optical Hilbert transformer has a simpler structure, a wider bandwidth and smaller amplitude and phase imbalance compared to the reported delay line based Hilbert transformer [15]. It also eliminates the use of an expensive and bulky FD-OP in the reported microwave photonic Hilbert transformer [16].

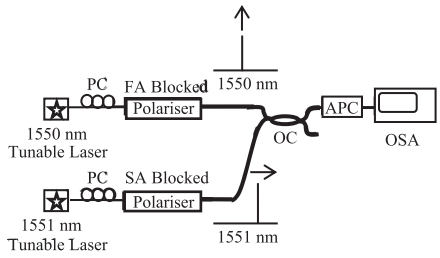

Fig. 4. Experimental setup to verify the APC has the function of independent control on the amplitude of two orthogonal linearly polarised light. The bold lines represent polarisation maintaining components. PC: polarisation controller; FA: fast axis; SA: slow axis; OC: optical coupler; APC: amplitude and phase controller; OSA: optical spectrum analyser.

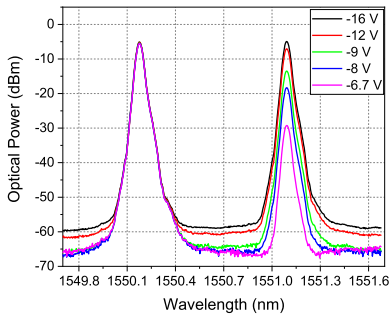

Fig. 5. Measured APC output optical spectrum for different DC voltage V_{DC3} into the bottom DDMZM inside the APC. The 1550 nm CW light was aligned to the slow axis and the 1551 nm CW light was aligned to the fast axis before launching into the APC.

III. Experimental Results

An experiment was set up as shown in Fig. 4 to verify the APC has the function of controlling the amplitude of the light in one polarisation state without affecting the amplitude of the light travelling in the orthogonal polarisation state. Two tunable lasers (Santec WSL-100 and Keysight N7711A) were employed to generate continuous wave (CW) light at 1550 nm and 1551 nm. Each of the two light waves passed through a polarisation controller (PC) followed by an in-line polariser. The PCs were adjusted so that the 1550 nm and 1551 nm CW light travelled in the slow and fast axis respectively after the polariser. The two different-wavelength orthogonal linearly polarised light were combined by a polarisation maintaining 50:50 optical coupler and launched into the APC implemented by a reverse operating DPol-DDMZM (Fujitsu FTM7980). All RF ports of the reverse operating DPol-DDMZM were terminated by 50 Ω terminators. A DC voltage V_{DC3} from a DC power supply was applied to the DC port of the bottom DDMZM. Fig. 5 shows the APC output optical spectrum measured on an optical spectrum analyser (Anritsu MS9740A) for difference V_{DC3}. It can be seen from the figure that the amplitude of the 1551 nm X-polarisation light in fast axis changes as V_{DC3} changes. On the other hand, the amplitude of the 1550 nm Y-polarisation light in slow axis

remains unchanged. A 24.3 dB optical power attenuation in the X-polarisation light was obtained by changing V_{DC3} from -16 V to -6.7 V.

An experiment was set up to verify broadband RF phase shifting operation can be obtained using the proposed APC. The setup consists of a tunable laser (Keysight N7711A), a DPol-DDMZM (Fujitsu FTM7980EDA) and an optical bandpass filter (OBPF) (Alnair Lab BVF-300CL) as shown in the dashed box in Fig. 3. The tunable laser generated a 1550 nm CW light with 13 dBm optical power. The top DDMZM in the DPol-DDMZM was driven by an RF signal and was biased at the null point, and the bottom DDMZM was biased at the peak point, as was discussed in Section II. The OBPF at the DPol-DDMZM output filtered out the lower RF modulation sideband. This produced orthogonal linearly polarised optical carrier and upper RF modulation sideband. They passed through a PC, which was used to align the polarisation state of the optical carrier and the upper RF modulation sideband to the fast and slow axis respectively before launching into the APC. The PC can be avoided by using polarisation maintaining components between the two DPol-DDMZMs. An erbium doped fibre amplifier (EDFA) (Amonics AEDFA-PA-35) and a 0.5 nm 3-dB bandwidth optical filter were connected to the APC output to compensate for the system loss and to suppress the amplified spontaneous emission noise. The output optical signal was detected by a photodetector (Discovery Semiconductor DSC30S) whose output was connected to an 18 GHz bandwidth network analyser (NA) (Keysight E5063A) to view the system amplitude and phase responses.

The bottom DDMZM in the APC was biased at the peak point to minimise the loss of the optical carrier passing through the APC. The system output phase response shown on the NA was calibrated to 0° when the DC voltage V_{DC1} into the two RF ports of the top DDMZM in the APC was -2 V. The phase and amplitude response of the APC were measured on the NA for different V_{DC1}. Fig. 6(a) shows $-180°$ to 180° RF signal phase shift is obtained by changing V_{DC1} from -2 V to 1.3 V. This shows a total of 3.3 V change in the DC voltage, which is close to twice the DDMZM RF port switching voltage of 1.7 V [18], is needed to obtain a full 360° phase shift. On the other hand, a total of 9.2 V DC voltage into a phase modulator with a polarisation dependent switching voltage is needed in the reported microwave photonic phase shifter [7]. The phase responses are flat over the 4 to 18 GHz frequency range. The system output amplitude response for different V_{DC1} are shown in Fig. 6(b). It can be seen from the figure that the change in the output RF signal amplitude is within -1 to 2 dB for 0° to 360° phase shift. The output RF signal amplitude change can be compensated by adjusting the bias angle β_3.

The new all-optical microwave photonic Hilbert transformer shown in Fig. 3 was set up. As in the above RF phase shifter experiment, the output of the DPol-DDMZM had an optical carrier in the fast axis and two RF modulation sidebands in the slow axis. They were amplified by an EDFA before filtering out the lower RF modulation sideband via the OBPF (Alnair Lab BVF-300CL). A 50:50 optical coupler was used to split the optical signal into two. One of the optical coupler outputs was connected to a PC followed by the APC. The PC was

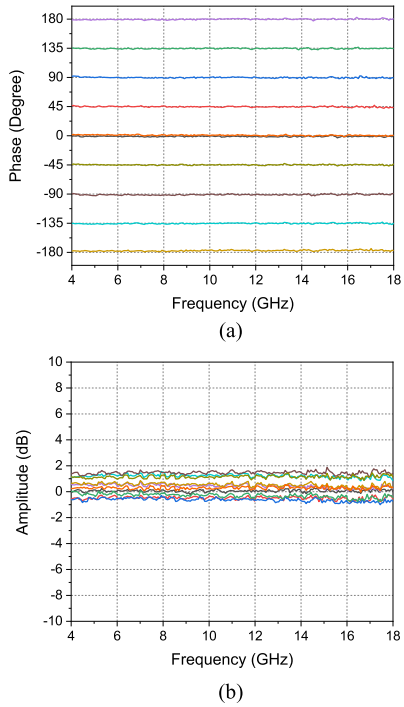

Fig. 6. Measured (a) phase and (b) amplitude response of the APC for different DC voltage V_{DC1} into the top DDMZM inside the APC.

adjusted to ensure the optical carrier and sideband travelled in the fast and slow axis respectively before launching into the reverse operating DPol-DDMZM. The other output of the optical coupler was connected to a PC followed by an in-line polariser, which converts the orthogonally polarised optical carrier and sideband to have the same polarisation state. Note that the PCs can be avoided by using polarisation maintaining components between the DPol-DDMZM and the APC/polariser. A variable optical attenuator and a variable delay line were connected after the polariser. They were used to match the optical power and the length in the two paths between the optical coupler and the photodetectors. The phase response measured on the NA connected to PD_2 output was calibrated to 0°. The phase response at PD_1 output was then measured on the NA for a DC voltage V_{DC1} of -0.4 V into the APC.

Fig. 7 shows the phase and amplitude responses measured at the two photodetector outputs. It can be seen from the figure that the phase response was flat with less than 2.5° phase imbalance over the 4 to 18 GHz frequency range. The amplitude response was also flat with less than 0.4 dB ripples. This verifies the two outputs of the Hilbert transformer have a $90° \pm 2.5°$ phase difference with little phase and amplitude imbalance. Note that, due to the NA used in the experiment has a limited bandwidth, two quadrature-phase outputs up to 18 GHz can only be demonstrated. It is important to note that the proposed all-optical Hilbert transformer can be operated at high frequencies. The upper operating frequency is only limited by the optical modulator bandwidth as the structure does not require high-frequency electrical components. For comparison, the delay line based Hilbert transformer has $\pm 5°$ phase imbalance and

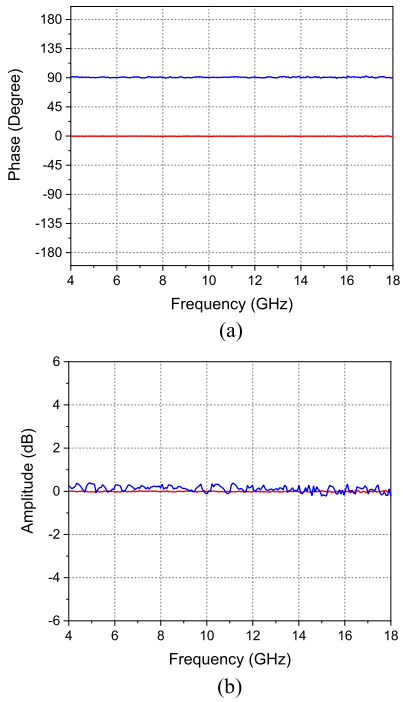

Fig. 7. Measured (a) phase and (b) amplitude response of the new all-optical Hilbert transformer. Responses at PD_2 output (red line) and PD_1 output (blue line) when $V_{DC1} = -0.4$ V.

3 dB amplitude ripples in a 2.4–17.6 GHz frequency range [15] and a commercial 4–18 GHz 90° hybrid coupler has a maximum amplitude and phase imbalance of ± 2 dB and $\pm 9°$ respectively [19]. This shows the all-optical microwave photonic Hilbert transformer has an excellent amplitude and phase imbalance performance.

IV. Conclusion

A new technique based on operating a DPol-DDMZM in reverse direction to realise independent amplitude and phase control of two orthogonal linearly polarised light have been presented. The phase of the Y-polarisation input light is controlled by the same DC voltage V_{DC1} into the two RF ports of a peak-biased DDMZM inside the APC. The amplitude of the X-polarisation input light is controlled by a DC voltage V_{DC3} into the DC port of the other DDMZM inside the APC. Changing V_{DC1} and V_{DC3} do not affect the light travelled in the orthogonal polarisation state. A new microwave photonic Hilbert transformer has been developed based on the proposed APC. Thanks to the all-optical structure, the Hilbert transformer has a wide bandwidth. Experiments have been conducted to verify the APC. The results show adjusting V_{DC3} can introduce 0–24.3 dB attenuation to the X-polarisation input light with no change in the Y-polarisation input light. A 0°–360° RF signal phase shift has been demonstrated by only a total of 3.3 V change in V_{DC1}, which is around 3 times less than that required in the RF phase shifter based on applying a DC voltage into a phase modulator. Two quadrature-phase outputs with less than 2.5° phase imbalance and 0.4 dB amplitude imbalance over a 4–18 GHz frequency range has also been demonstrated using the APC to implement an all-optical Hilbert transformer.

References

[1] R. A. Minasian, E. H. W. Chan, and X. Yi, "Microwave photonic signal processing," *Opt. Exp.*, vol. 21, no. 19, pp. 22918–22936, 2013.
[2] X. Zou, B. Lu, W. Pan, L. Yan, A. Stohr, and J. Yao, "Photonics for microwave measurements," *Laser Photon. Rev.*, vol. 10, no. 5, pp. 711–734, 2016.
[3] B. M. Haas and T. E. Murphy, "A simple, linearized, phase-modulated analog optical transmission system," *IEEE Photon. Technol. Lett.*, vol. 19, no. 10, pp. 729–731, May 2007.
[4] R. Zheng, E. H. W. Chan, X. Wang, X. Feng, and B. Guan, "Broadband high dynamic range fiber optic link based on a dual-polarization modulator," *Opt. Exp.*, vol. 27, no. 4, pp. 4734–4747, 2019.
[5] C. Huang, H. Chen, and E. H. W. Chan, "Microwave photonic frequency tripler based on an integrated dual-parallel modulator structure," *IEEE Photon. J.*, vol. 9, no. 5, Oct. 2017, Art. no. 7204010.
[6] Y. Zhang and S. Pan, "Broadband microwave signal processing enabled by polarization-based photonic microwave phase shifters," *IEEE J. Quantum Electron.*, vol. 54, no. 4, pp. 1–12, Aug. 2018.
[7] T. Li, E. H. W. Chan, X. Wang, X. Feng, and B. Guan, "All-optical photonic microwave phase shifter requiring only a single DC voltage control," *IEEE Photon. J.*, vol. 8, no. 4, Aug. 2016, Art. no. 5501008.
[8] K. P. Ho and H. W. Cuei, "Generation of arbitrary quadrature signals using one dual-drive modulator," *J. Lightw. Technol.*, vol. 23, no. 2, pp. 764–770, 2005.
[9] C. Huang and E. H. W. Chan, "Photonics-based serrodyne microwave frequency translator with large spurious suppression and phase shifting capability," *J. Lightw. Technol.*, vol. 39, no. 7, pp. 2052–2058, 2021.
[10] G. K. Gopalakrishnan, W. K. Burns, R. W. McElhanon, C. H. Bulmer, and A. S. Greenblatt, "Performance and modeling of broadband linbO_3 traveling wave optical intensity modulators," *J. Lightw. Technol.*, vol. 12, no. 10, pp. 1807–1818, 1994.
[11] C. Huang and E. H. W. Chan, "Variable optical attenuators with ability to independently control two orthogonal linearly polarised light amplitudes," *Chin. Opt. Lett.*, vol. 16, no. 4, 2018, Art. no. 042301.
[12] Z. Peng, A. Wen, Y. Gao, and Z. Tu, "A tunable and wideband microwave photonic phase shifter based on dual-polarization modulator," *Opt. Commun.*, vol. 382, pp. 377–380, 2017.
[13] R. Zheng, E. H. W. Chan, X. Wang, X. Feng, and B. Guan, "Microwave photonic devices based on liquid crystal on silicon technology," *Appl. Sci., Special Issue Microw. Photon.*, vol. 9, no. 2, 2019, Art. no. 260.
[14] E. L. Wooten *et al.*, "A review of lithium niobate modulators for fiber-optic communication systems," *IEEE J. Sel. Topics Quantum Electron.*, vol. 6, no. 1, pp. 69–82, Jan./Feb. 2000.
[15] H. Emami, N. Sarkhosh, L. Bui, and A. Mitchell, "Wideband RF photonic in-phase and quadrature-phase generation," *Opt. Lett.*, vol. 33, no. 2, pp. 98–100, 2008.
[16] Y. Cao, E. H. W. Chan, X. Wang, X. Feng, and B. Guan, "Photonic microwave quadrature filter with low phase imbalance and high signal-to-noise ratio performance," *Opt. Lett.*, vol. 40, no. 20, pp. 4663–4666, 2015.
[17] T. Kawanishi, S. Shinada, T. Sakamoto, S. Oikawa, K. Yoshiara, and M. Izutsu, "Reciprocating optical modulator with resonant modulating electrode," *Electron. Lett.*, vol. 41, no. 5, pp. 271–272, 2005.
[18] X. Wang, T. Niu, E. H. W. Chan, X. Feng, B. Guan, and J. Yao, "Photonics-based wideband microwave phase shifter," *IEEE Photon. J.*, vol. 9, no. 3, Jun. 2017, Art. no. 5501710.
[19] Marki Microwave, "4-18 GHz 90° splitter /combiner MQS-0418 datasheet," 2018. [Online]. Available: http://www.markimicrowave.com